ISSN 0915-633X

INTERNATIONAL ATOMIC ENERGY AGENCY

SIXTEENTH IAEA FUSION ENERGY CONFERENCE

Montréal, Canada, 7-11 October 1996

IAEA-CN-64/G2-4

NATIONAL INSTITUTE FOR FUSION SCIENCE

Superconducting Magnet Design and Construction of LHD

O. Motojima, N. Yanagi, S. Imagawa, K. Takahata, S. Yamada, A. Iwamoto, H. Chikaraishi, S. Kitagawa, R. Maekawa, S. Masuzaki, T. Mito, T. Morisaki, A. Nishimura, S. Sakakibara, S. Satoh, T. Satow, H. Tamura, S. Tanahashi, K. Watanabe, S. Yamaguchi, J. Yamamoto, M.Fujiwara and A. Iiyoshi

(Received - Aug. 30, 1996)

NIFS-445 Sep. 1996

RESEARCH REPORT
NIFS Series

NAGOYA, JAPAN

F1-CN-64/G2-4

SUPERCONDUCTING MAGNET DESIGN AND CONSTRUCTION OF LHD

O.MOTOJIMA, N.YANAGI, S.IMAGAWA, K.TAKAHATA, S.YAMADA,
A.IWAMOTO, H.CHIKARAISHI, S.KITAGAWA, R.MAEKAWA, S.MASUZAKI,
T.MITO, T.MORISAKI, A.NISHIMURA, S.SAKAKIBARA, S.SATOH,
T.SATOW, H.TAMURA, S.TANAHASHI, K.WATANABE, S.YAMAGUCHI,
J.YAMAMOTO, M.FUJIWARA, and A.IIYOSHI

National Institute for Fusion Science
322-6 Oroshicho, Toki 509-52, Japan

KEYWORD : Large Helical Device, LHD, currentless toroidal system, superconducting coil, helical coil, poloidal coil, SC bus line, divertor, disruption free system

ABSTRACT

The Large Helical Device project is now successfully executing its 7th year program of 8 years construction period. Superconducting (SC) Research and Development tasks for the LHD SC coil construction have been already completed, and we have now accomplished more than 75% of the whole construction schedule. In this paper, we report the recent progress of SC R&D obtained, and the fabrication technology developed for a huge and reliable SC coil system. These results are applicable to a future experimental reactor in the next decade with a much larger SC coil system.

The LHD is called heliotron and has $\ell/m = 2/10$ SC helical coils and three sets of SC poloidal coils, of which coil currents are 7.8 MA, 5.0 MA, -4.5 MA, and -4.5 MA, respectively. The major radius, minor helical coil radius, minor plasma radius, and plasma volume are 3.9 m, 0.975 m, 0.5~0.65 m, and 20~30 m^3, respectively. In addition to an SC coil system, the main body of the LHD consists of huge supporting structures for the electromagnetic force, a vacuum chamber, an outer cryostat, and a machine base. The total weight is about 1,500 tons, in which LHe cooled mass is 850 tons. The LHD has a maximum stored energy of 1.6 GJ (4 T at the plasma center). The major goal of the LHD project is to demonstrate the high potentiality of the helical-type device producing current-less-steady-state plasmas with an enough large Lawson parameter in absence of any danger of a plasma current-disruption. It provides a useful and reliable data base making it possible to predict a fusion reactor condition. The realization of the steady-state operation requires a large extent of engineering innovations, primarily in the areas of superconducting technology, plasma facing materials and water cooling systems, and heating systems. It also contributes to building up the engineering scenario required for a long-pulse regulated plasma operation necessary for the fusion research.

1. INTRODUCTION

The LHD, a heliotron-type apparatus, is a superconducting toroidal device with a major radius of 3.9 m. It has $\ell/m = 2/10$ SC helical coils and three sets of SC poloidal coils, of which coil currents are 7.8 MA, 5.0 MA, -4.5 MA, and -4.5 MA, respectively. The major goal of the LHD project is to demonstrate a high potentiality of the heliotron-type device producing currentless steady-state plasmas with an enough large Lawson parameter and without any danger of a plasma current disruption. The SC is a key technology of the LHD project. The schematic view and the specification of the LHD are shown in Fig.1 and in Table 1. In Table 2, the parameters of the LHD SC coils are listed. Both helical and OV poloidal coils are the largest SC coils among the existing fusion devices.

The main objectives and target parameters of the LHD[1,2,3] are (1) confinement studies and the demonstration of high temperature plasmas such as the density $\langle n \rangle = 10^{20}$ m^{-3} and the temperature $\langle T \rangle$ = 3-4 keV, or $\langle n \rangle = 2 \times 10^{19}$ m^{-3} and T(0) = 10 keV under an input heating power of 20 MW, (2) MHD studies and the realization of high beta plasmas $\langle \beta \rangle \geq 5\%$, (3) studies on confinement improvement and steady-state experiments by a divertor, and (4) developments on physics and technologies for a fusion reactor. The realization of the steady-state operation requires a large extent of engineering innovations, primarily in the areas of superconducting technology, plasma facing materials and water cooling systems, and heating systems. It also contributes to building up the engineering scenario for a long-pulse regulated plasma operation. In this paper, we generally review the major progress of the LHD project, i.e., the present status of construction, recent progress of SC R&D obtained, and the fabrication technique developed for the construction of the large and reliable SC magnet system. These are the necessary goals of the LHD project and are expected to contribute to a future experimental reactor in the next decade.

The LHD project is now successfully executing 7th year program of 8 years construction. The engineering research and development for the LHD have almost been completed, and we have now accomplished more than 75% of the tough and long construction schedule.

2. SC MAGNET TECHNOLOGY

In this section, we elucidate the new SC magnet technology developed in NIFS to execute the LHD construction, which are 1) development of helical and poloidal coil conductors, 2) fabrication technique, 3) test procedure and quality control, 4) mechanical design, and 5) bus lines, etc.

2.1 DEVELOPMENT OF HELICAL COIL CONDUCTOR AND TEST PROCEDURE

Many types of superconductors with different internal structures were proposed and examined practically with short sample tests[4]. The final conductor size is 12.5 mm x 18.0 mm, and the nominal current is 13.0 kA (4.4K/Phase I, 17.3 kA for 1.8K/Phase II). The main specification of the superconductor is listed in Table 2 and the cross-sectional configuration is shown in Fig. 2. The pure aluminum (5 nine) is the main stabilizer. The conductor size has been optimized not only for the mechanical flexibility to facilitate the on-site winding process but also for the cryogenic stability due to the increment of the surface/volume ratio. Fifteen NbTi superconducting strands are twisted and formed into a Rutherford-type flat cable. Instead of the conventional OFCu, Cu-2%Ni (resistivity: $\sim 2.5 \times 10^{-9}$ Ω m) was selected for the clad material around

the aluminum to insulate the Hall current[5] while maintaining the smooth current transfer from the superconducting strands to the aluminum. Another important development of the conductor is the adoption of the electron beam welding to the half-hard copper sheath, which has drastically enhanced the mechanical toughness of the conductor not only against the compressional stress of up to 100 MPa during the excitation but also against the plastic deformation during the three dimensional winding process. The conductor surface is oxidized to improve the heat transfer to the liquid helium.

The total length of more than 36 km have been fabricated with a unit length of 600～1100 m, wound in 38 bobbins. Each unit produced has been carefully inspected for necessary items, such as the critical current of the strands, the resistivity of the pure aluminum, the mechanical toughness and the heat transfer coefficient. Short sample tests have been carried out to evaluate the basic properties of each superconductor, using the test facilities with 9 T split coils, 100 kA current leads and 75 kA DC power supplies.

Figure 3 shows obtained critical currents and recovery currents for all conductors as a function of the bias magnetic field. The critical current shows a good agreement with the value predicted by integrating the critical current of each single strand, taking account of the three dimensional self-field effect. The scattering of critical currents is in the range of 4% at 7 T. Stability tests have also been carried out by initiating a normal zone with heaters and by measuring the recovery current. It should be noted that recovery currents exceeded the nominal current value for the 4.4K operating condition (13.0 kA at 6.9 T).

2.1.1 MECHANICAL REQUIREMENT FOR HELICAL COIL

The fabrication error for the coil position is required to be under 2 mm that corresponds to 5×10^{-4} of the major radius[5]. Furthermore, the elastic deformation of the coil by electromagnetic force is specified to be under 1.9 mm at 3 T operation. The helical coil conductors are, therefore, designed to be packed into a thick coil-can made of stainless steel SUS316. Since the coil-can is used as a bobbin for winding, it must be fabricated with a high accuracy. A torus-shaped winding core was, therefore, prepared with high accuracy of 0.2 mm. The top or bottom half pitch of the coil-can was manufactured with NC machinery in a factory. These parts were assembled and welded with each other in Toki site. As the results of R&D for the new welding technique, the fabrication error of the coil-can has been made enough small for the adequate helical coil winding. The movement and the stress of each conductor were calculated by using ANSYS 4.4 as shown in Fig. 4. The electromagnetic force is applied to the node which is the center of each conductor. Since the insulators between conductors are separated, the compressive Young's modulus is calculated multiplying the actual value by a spacer factor. The Young's modulus (E) along the conductor is negligibly small. Inner materials of the composite conductor, which are superconducting strands, CuNi clad pure aluminum and solder, are represented by homogeneous elements.

We have developed a new GFRP insulator with high rigidity. The Young's modulus is larger than 22 GPa, and the compressive strength is over 1000 MPa. In the case of the rigidity of 22 GPa and the spacer factor of 0.5, the movement of the bottom layer and the maximum stress on conductors are calculated to be 1.1 mm and 173 MPa, respectively. In this analysis, the averaged Young's

modulus of the stabilizer and SC strands (E_{Al+sc}) is given as 10 GPa. Since the fabrication gap between conductors and insulators is expected to be crushed by a large electromagnetic force, the equivalent rigidity of the coil is reduced simultaneously. This effect was estimated by assuming that the total gaps are equal to the increment of the displacement of the bottom layer. The result is shown in Fig. 5. The larger the gap is, the higher the stress on the conductor is. The stress on the aluminum in the top layers is below the yield strength. This means that it is a reasonable assumption that E_{Al+sc} is 10 GPa. The fabrication gap averaged has been established to be within 65 μ m/layer to keep the stress on the conductor under the yield strength. We are able to avoid the quench caused by plastic deformation of the conductors.

2.2 POLOIDAL COIL DEVELOPMENT

To fabricate the poloidal coils, a forced flow cooled conductor with a high stability margin (NbTi cable in conduit type, Table 2) has been developed to reduce the AC loss due to the coil current shift during the plasma experiments (about 1 kA/sec). Cool-down and current-excitation tests on the smallest poloidal coil (inner vertical coil, IV coil) was a highlight of the poloidal coil R&D in 1995[7]. Without experiencing any coil quench, we could raise the current to the nominal value of 20.8 kA.

2.2.1 POLOIDAL COIL CONFIGURATION

The poloidal coils consist of Inner Vertical (IV), Inner Shaping (IS) and Outer Vertical (OV) coils. The IV and IS coils have been completed in the factory and shipped to the institute. The on-site winding of OV coils has been finished, and lower three coils have already been installed into a lower part of the LHD supporting structure.

The NbTi cable-in-conduit conductors are adopted because of its high stability. The specifications are listed in Table 2. The void fraction is 0.38, which is optimized from the viewpoint of the strand movement and inter-strand coupling losses. The strand surface is uncoated. Taking care of the current distribution and the heat transfer to the helium, we confirmed that a bare strand provided a high stability margin. The critical current was set to be three times as high as the operating current at the maximum field. The previous research also suggested that the stability for partial quench was enhanced when the critical current was more than twice as high as the operating current.

An important subject of the design and fabrication is to reduce the error field from the poloidal coils. The required accuracy is 1×10^{-4} at the plasma surface. To minimize the error field, the molded pancakes kept tolerances of ±2 mm for the inner and outer diameters and ±1 mm for the height. The tolerances correspond to the extreme accuracy of about 5×10^{-4} for the diameter. As for the electric joints between pancakes, a solid state bonding method was applied. The NbTi filaments were jointed trying to keep their superconductive performances. The required space for the joint is only 37 mm wide, 50 mm high and 60 mm long. The joint was small enough to reduce the error field.

2.2.2 PERFORMANCE TEST OF IV COIL

One of the IV coils was set in a single-coil-testing cryostat and connected to the test facilities in NIFS. The helium refrigerator capacity is 600 W at 4.4K or 250 l/h. The inlet gas temperature was controlled by mixing cool ($\sim$80K) and

hot (~280K) gases from the cold box. The temperature difference between the inlet and outlet was then kept less than 50K. Following the initial cooling phase, the steady cooling was carried out with a supercritical helium centrifugal pump. The specified mass flow rate was 50 g/s, and the inlet pressure was about 0.9 MPa. The pressure drop was measured during cool-down and steady cooling. An extended summary of the results of the single cool down and excitation tests of an IV coil is as follows. (1) The total cool down time was about 250 hours. (2) The coil contracted uniformly by the design value, about 6 mm. (3) The relationship between the friction factor and the Reynolds number in the cool down phase agreed well with the results obtained by the R&D coils previously tested. (4) The friction factor decreased by increasing the operating current, which might be explained by the produced narrow gap inside the conduit due to the electromagnetic force. (5) The coil was successfully energized up to the specified current in spite of the deformation of the strands bundle. The conductor possessed the high stability margin. (6) The heat generation of a joint was 0.06 W at 20.8 kA, which was negligible for conductor stability. (7) The radial displacement and acoustic emission observed suggested that the coil was mechanically stable.

2.3 SC BUS-LINE SYSTEM

A superconducting flexible bus-line has been developed for a current feed system for the LHD. An aluminum stabilized NbTi/Cu compacted strand cable is used to satisfy the requirement for the fully stabilized condition at the nominal current of 32 kA. We will utilize the SC bus-lines for both helical and poloidal coils. The bus-line system is shown in Fig. 6.

The design concepts for an SC current feeder system for the LHD are as follows. (1) Fully stabilized SC properties should be satisfied for the nominal current of 31.3 kA (for OV coils). (2) The breakdown voltage should be higher than that of the SC coils. (3) The system should be able to maintain its rated current carrying capacities for 30 minutes, even if the coolants supplied to the current feeder system are stopped. The SC current feeder system is required to have enough safety margin exceeding those of the SC coils, because the stored magnetic energy of the coils must be extracted through the SC bus-lines when the coils quench. The SC bus-lines should be flexible since the routes from coils to their power supplies have many corners. The minimum bend radius is designed to be 1.5 m, because of the restriction on the height, and width. The design specifications for the SC bus-lines are listed in Table 3.

We have manufactured a full scale model of a 20 m long SC bus-line which is shown in Fig. 7[8]. Performance tests of the full scale model were successfully carried out. A minimum propagation current for the normal transition larger than 32.5 kA was observed when a perturbation energy of 80 J was added. We also successfully conducted an over-current operation up to 40 kA without any quench. The current distribution among the SC strands was investigated for ramp rates from 100 A/s to 2 kA/s, and the deviation of the distributed currents was less than 7%. The heat load into the returned cold helium gas in the corrugated transfer line was 4.55 W/m.

The breakdown voltage between +/- cables was measured with test pieces of R&D SC cables of 150 mm in length. Both ends of the test pieces were covered by electrical insulators. Tests were conducted over a wide range of the temperature from 4.2 to 294K using helium gas. In the coil protection circuits of

LHD, the maximum induced voltage of the coils is 1.9 kV in the case of the decay time constant of 20 s. The insulation structure of the SC cables has a large breakdown voltage margin more than 20 kV at the LHe temperature.

3. SUMMARY

Experiencing the R&Ds, the engineering design, and the construction of the LHD, we have developed the various amount of SC magnet technologies which are contributing to the development in the fusion technology area.

In the following, we briefly discuss further information on the major progress of the SC magnet technology during the LHD construction. (1) Helical coil conductor joints; there are 32 joints, in which we could obtain enough low value of the resistance of each joint less than 0.7 nΩ (0.2 W at 17.3 kA). (2) Evaluation of the AC loss in the helical coil conductor; the AC loss of the helical coil conductor is evaluated by applying a time-varying magnetic field. From the magnetization of the conductor, the time constant of 4.3 sec was obtained. (3) Coil protection; the coil protection circuit for the helical and poloidal coil system is an urgent subject for the LHD operation. A 30 kA range of DC circuit breaker using a power fuse and an AC vacuum breaker has been developed for this circuit with a dump resistor. After the demonstration tests using the practical circuit and dummy coils, the operation sequence and the possibility of fault of less than 5×10^{-3} have been confirmed. (4) A supercritical helium pump for the forced flow cooling; an SHe circulating pump for poloidal coils has been developed and tested during the IV coil test (50 g/s). The mechanical performance with the high pressure drop between the inlet and the outlet (1 atm) was confirmed.

In this year, 1996, the major activity of the LHD construction will move to the finalizing phase at the Toki site. The completion of the construction schedule is at the end of 1997. We will keep continuing the necessary tasks for the construction and the assembly of the LHD, which will be completed almost within one and half a years from now, and then the first plasma experiment will start.

REFERENCES

1. O.Motojima, Fusion Technology 26 (1994) 437
2. O.Motojima, Symposium on Fusion Engineering, Champaign, Ill., September 30-October 5, 1995, Invited
3. O.Motojima, et al., Fusion Technology 27 (1995) 123
4. T.Mito, et al., Fusion Engineering Design 10 (1993) 233
5. N.Yanagi, et al., Advances in Cryogenic Engineering-Materials 40 (1994) 459
6. K.Yamazaki, et al., Fusion Energy Design 10 (1993) 79
7. T.Satow, et al., presented at ICEC16, Kitakyushu, Japan (May 21-24) OA7-3
8. S.Yamada, et al., 18th Symposium on Fusion Technology, 1994, Karlsruhe, D-425

Table 1. Specifications of LHD

Major Radius	3.9 m
Averaged Plasma Radius	0.5～0.65 m
ℓ, m	2, 10
Magnetic Field	3(4) T
Helical Coil Current	5.85(7.8) MA
Coil Minor Radius	0.975 m
LHc Temperature	4.4(1.8) K
Poloidal Coil Current	
Inner Vertical Coil	5.0 MA
Inner Shaping Coil	-4.5 MA
Outer Vertical Coil	-4.5 MA
LHe Temperature	4.5 K
Plasma Volume	20～30 m^3
Heating Power	40 MW
Coil Energy	0.9(1.6) GJ
Refrigeration Power	9(～15) kW

Table 3 Specifications of SC Bus-Line

Items	Specification
Number	6 (Helical Coils)
	3 (Poloidal Coils)
Rated Current	32 kA
Rated Voltage	5.7 kV (80 K GHe)
Length	45 - 65 m
Min. Bending Radius	1.5 m
Heat Load	0.3 W/m (80-4.2 K)
	3 W/m (300-80 K)
Type	Five Corrugated Tubes

Table 2 List of Coil Parameters

Items	Helical Coil	IV Coil	IS Coil	OV Coil
Superconductor	NbTi/Cu	<--	<--	<--
Conductor Type	Compacted Strands CICC		<--	<--
Cooling Method	Pool-Cooled	Forced Flow	<--	<--
Conductor Size	12.5x18.0 mm	23.0x27.6	23.0x27.6	27.5x31.8
Major Radius	3.9 m	1.80	2.82	5.55
Weight per Coil	120 tons	16	25	50
Maximum Field in Coil	9.2 T	6.5	5.4	5.0
Stored Energy	1.6 GJ	0.16	0.22	0.61
Nominal Current	17.3 kA	20.8	21.6	31.3
Coil Current Density	53 A/mm2	29.8	31.5	33.0
Magnetomotive Force	7.8 MA	5.0	-4.5	-4.5
Hoop Force	356 MN	262	116	263
Up-down Force	240 MN	-60.2	95.6	72.2
Diameter of Filament	47 μ m	15	12	14
Diameter of Strand	1.74mm	0.76	0.76	0.89
Number of Strands	15	486	<--	<--

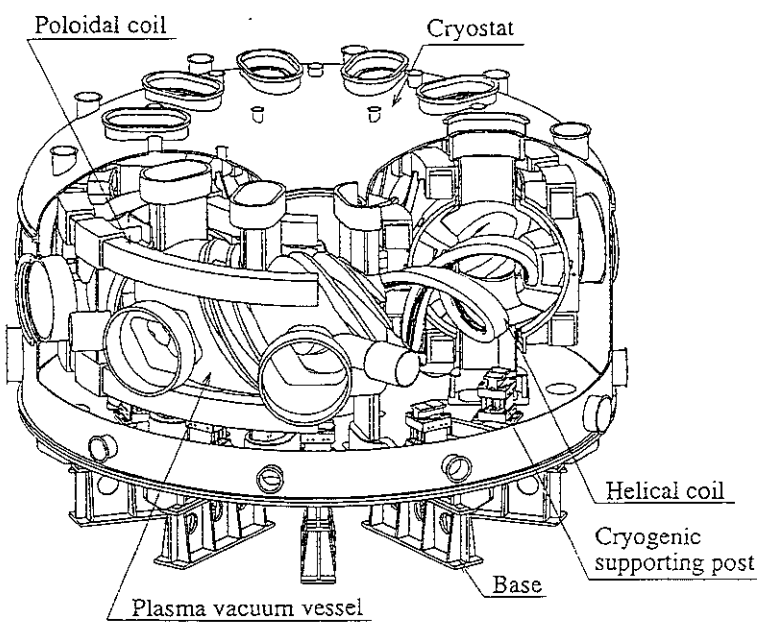

Fig. 1 Bird's Eye View of LHD

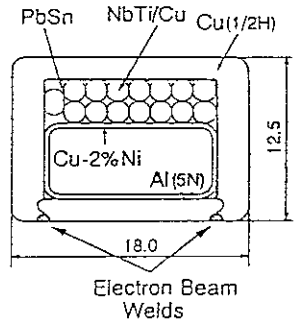

Fig. 2. Coss-sectional view of the superconductor.

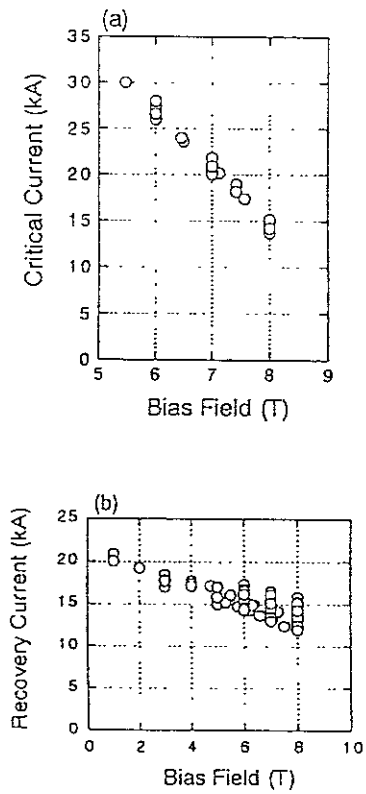

Fig. 3. (a) Critical currents and (b) recovery currents vs. bias magnetic fields for all short samples.

NIFS-420 Y.N. Nejoh,
Arbitrary Amplitude Ion-acoustic Waves in a Relativistic Electron-beam Plasma System; July 1996

NIFS-421 K. Kondo, K. Ida, C. Christou, V.Yu.Sergeev, K.V.Khlopenkov, S.Sudo, F. Sano, H. Zushi, T. Mizuuchi, S. Besshou, H. Okada, K. Nagasaki, K. Sakamoto, Y. Kurimoto, H. Funaba, T. Hamada, T. Kinoshita, S. Kado, Y. Kanda, T. Okamoto, M. Wakatani and T. Obiki,
Behavior of Pellet Injected Li Ions into Heliotron E Plasmas; July 1996

NIFS-422 Y. Kondoh, M. Yamaguchi and K. Yokozuka,
Simulations of Toroidal Current Drive without External Magnetic Helicity Injection; July 1996

NIFS-423 Joong-San Koog,
Development of an Imaging VUV Monochromator in Normal Incidence Region; July 1996

NIFS-424 K. Orito,
A New Technique Based on the Transformation of Variables for Nonlinear Drift and Rossby Vortices; July 1996

NIFS-425 A. Fujisawa, H. Iguchi, S. Lee, T.P. Crowley, Y. Hamada, H. Sanuki, K. Itoh, S. Kubo, H. Idei, T. Minami, K. Tanaka, K. Ida, S. Nishimura, S. Hidekuma, M. Kojima, C. Takahashi, S. Okamura and K. Matsuoka,
Direct Observation of Potential Profiles with a 200keV Heavy Ion Beam Probe and Evaluation of Loss Cone Structure in Toroidal Helical Plasmas on the Compact Helical System; July 1996

NIFS-426 H. Kitauchi, K. Araki and S. Kida,
Flow Structure of Thermal Convection in a Rotating Spherical Shell; July 1996

NIFS-427 S. Kida and S. Goto,
Lagrangian Direct-interaction Approximation for Homogeneous Isotropic Turbulence; July 1996

NIFS-428 V.Yu. Sergeev, K.V. Khlopenkov, B.V. Kuteev, S. Sudo, K. Kondo, F. Sano, H. Zushi, H. Okada, S. Besshou, T. Mizuuchi, K. Nagasaki, Y. Kurimoto and T. Obiki,
Recent Experiments on Li Pellet Injection into Heliotron E; Aug. 1996

NIFS-429 N. Noda, V. Philipps and R. Neu,
A Review of Recent Experiments on W and High Z Materials as Plasma-Facing Components in Magnetic Fusion Devices; Aug. 1996

NIFS-430 R.L. Tobler, A. Nishimura and J. Yamamoto,

Recent Issues of NIFS Series

NIFS-408 K. Hirose, S. Saito and Yoshi.H. Ichikawa
Structure of Period-2 Step-1 Accelerator Island in Area Preserving Maps; Mar. 1996

NIFS-409 G.Y.Yu, M. Okamoto, H. Sanuki, T. Amano,
Effect of Plasma Inertia on Vertical Displacement Instability in Tokamaks; Mar. 1996

NIFS-410 T. Yamagishi,
Solution of Initial Value Problem of Gyro-Kinetic Equation; Mar. 1996

NIFS-411 K. Ida and N. Nakajima,
Comparison of Parallel Viscosity with Neoclassical Theory; Apr. 1996

NIFS-412 T. Ohkawa and H. Ohkawa,
Cuspher, A Combined Confinement System; Apr. 1996

NIFS-413 Y. Nomura, Y.H. Ichikawa and A.T. Filippov,
Stochasticity in the Josephson Map; Apr. 1996

NIFS-414 J. Uramoto,
Production Mechanism of Negative Pionlike Particles in H_2 Gas Discharge Plasma; Apr. 1996

NIFS-415 A. Fujisawa, H. Iguchi, S. Lee, T.P. Crowley, Y. Hamada, S. Hidekuma, M. Kojima,
Active Trajectory Control for a Heavy Ion Beam Probe on the Compact Helical System; May 1996

NIFS-416 M. Iwase, K. Ohkubo, S. Kubo and H. Idei
Band Rejection Filter for Measurement of Electron Cyclotron Emission during Electron Cyclotron Heating; May 1996

NIFS-417 T. Yabe, H. Daido,T. Aoki, E. Matsunaga and K. Arisawa,
Anomalous Crater Formation in Pulsed-Laser-Illuminated Aluminum Slab and Debris Distribution; May 1996

NIFS-418 J. Uramoto,
Extraction of K^- Mesonlike Particles from a D_2 Gas Discharge Plasma in Magnetic Field; May 1996

NIFS-419 J. Xu, K. Toi, H. Kuramoto, A. Nishizawa, J. Fujita, A. Ejiri, K. Narihara, T. Seki, H. Sakakita, K. Kawahata, K. Ida, K. Adachi, R. Akiyama, Y. Hamada, S. Hirokura, Y. Kawasumi, M. Kojima, I. Nomura, S. Ohdachi, K.N. Sato
Measurement of Internal Magnetic Field with Motional Stark Polarimetry in Current Ramp-Up Experiments of JIPP T-IIU; June 1996

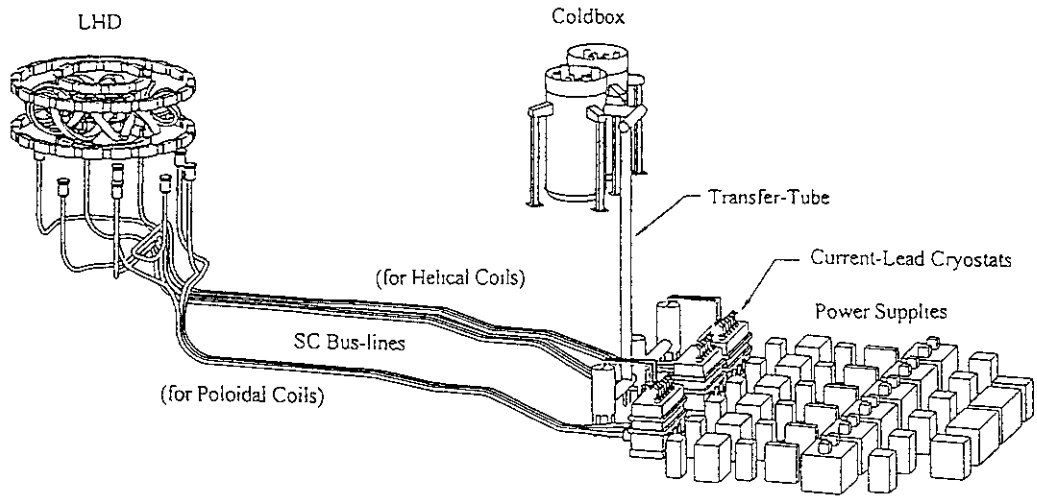

Fig. 6. Layout of the superconduting bus lines

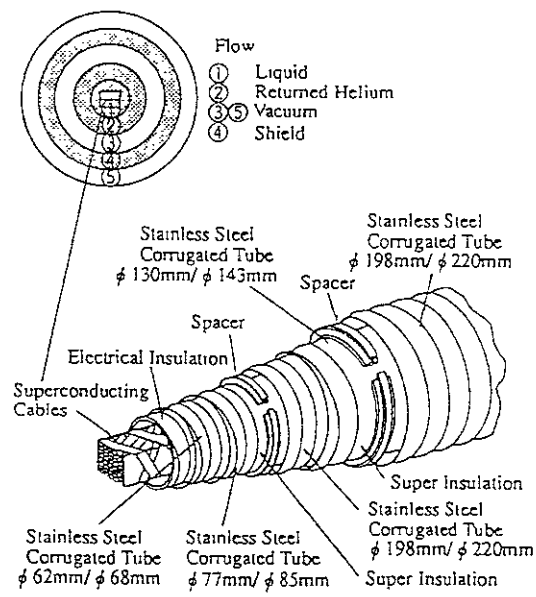

Fig. 7. Cross section of superconducting bus line.

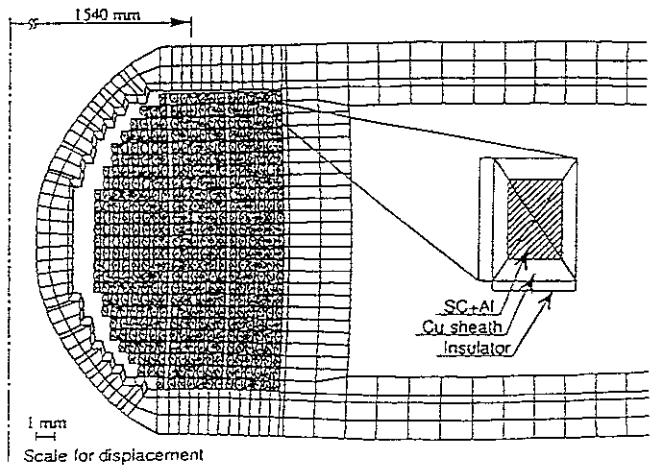

Fig. 4. Deformed shape of the helical coil where the rigidity of insulators and the spacer factor are 22 GPa and 0.5 constant, respectively.

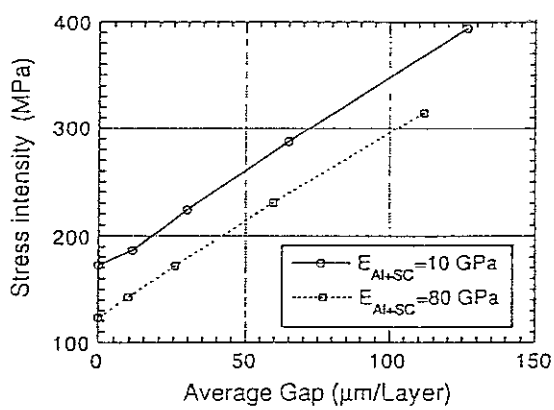

Fig. 5. Calculated maximum stress on conductors for various fabrication gaps where the Young's modulus of the insulator is 22 GPa.

Design-Relevant Mechanical Properties of 316-Type Stainless Steels for Superconducting Magnets; Aug. 1996

NIFS-431 K. Tsuzuki, M. Natsir, N. Inoue, A. Sagara, N. Noda, O. Motojima, T. Mochizuki, T. Hino and T. Yamashina,
Hydrogen Absorption Behavior into Boron Films by Glow Discharges in Hydrogen and Helium; Aug. 1996

NIFS-432 T.-H. Watanabe, T. Sato and T. Hayashi,
Magnetohydrodynamic Simulation on Co- and Counter-helicity Merging of Spheromaks and Driven Magnetic Reconnection; Aug. 1996

NIFS-433 R. Horiuchi and T. Sato,
Particle Simulation Study of Collisionless Driven Reconnection in a Sheared Magnetic Field; Aug. 1996

NIFS-434 Y. Suzuki, K. Kusano and K. Nishikawa,
Three-Dimensional Simulation Study of the Magnetohydrodynamic Relaxation Process in the Solar Corona. II.; Aug. 1996

NIFS-435 H. Sugama and W. Horton,
Transport Processes and Entropy Production in Toroidally Rotating Plasmas with Electrostatic Turbulence; Aug. 1996

NIFS-436 T. Kato, E. Rachlew-Källne, P. Hörling and K.-D Zastrow,
Observations and Modelling of Line Intensity Ratios of OV Multiplet Lines for 2s3s 3S1 - 2s3p 3Pj; Aug. 1996

NIFS-437 T. Morisaki, A. Komori, R. Akiyama, H. Idei, H. Iguchi, N. Inoue, Y. Kawai, S. Kubo, S. Masuzaki, K. Matsuoka, T. Minami, S. Morita, N. Noda, N. Ohyabu, S. Okamura, M. Osakabe, H. Suzuki, K. Tanaka, C. Takahashi, H. Yamada, I. Yamada and O. Motojima,
Experimental Study of Edge Plasma Structure in Various Discharges on Compact Helical System; Aug. 1996

NIFS-438 A. Komori, N. Ohyabu, S. Masuzaki, T. Morisaki, H. Suzuki, C. Takahashi, S. Sakakibara, K. Watanabe, T. Watanabe, T. Minami, S. Morita, K. Tanaka, S. Ohdachi, S. Kubo, N. Inoue, H. Yamada, K. Nishimura, S. Okamura, K. Matsuoka, O. Motojima, M. Fujiwara, A. Iiyoshi, C. C. Klepper, J.F. Lyon, A.C. England, D.E. Greenwood, D.K. Lee, D.R. Overbey, J.A. Rome, D.E. Schechter and C.T. Wilson,
Edge Plasma Control by a Local Island Divertor in the Compact Helical System; Sep. 1996 (IAEA-CN-64/C1-2)

NIFS-439 K. Ida, K. Kondo, K. Nagaski T. Hamada, H. Zushi, S. Hidekuma, F. Sano, T. Mizuuchi, H. Okada, S. Besshou, H. Funaba, Y. Kurimoto, K. Watanabe and T. Obiki,
Dynamics of Ion Temperature in Heliotron-E; Sep. 1996 (IAEA-CN-64/CP-5)

NIFS-440 S. Morita, H. Idei, H. Iguchi, S. Kubo, K. Matsuoka, T. Minami, S. Okamura, T. Ozaki, K. Tanaka, K. Toi, R. Akiyama, A. Ejiri, A. Fujisawa, M. Fujiwara, M. Goto, K. Ida, N. Inoue, A. Komori, R. Kumazawa, S. Masuzaki, T. Morisaki, S. Muto, K. Narihara, K. Nishimura, I. Nomura, S. Ohdachi, M.. Osakabe, A. Sagara, Y. Shirai, H. Suzuki, C. Takahashi, K. Tsumori, T. Watari, H. Yamada and I. Yamada,
A Study on Density Profile and Density Limit of NBI Plasmas in CHS; Sep. 1996 (IAEA-CN-64/CP-3)

NIFS-441 O. Kaneko, Y. Takeiri, K. Tsumori, Y. Oka, M. Osakabe, R. Akiyama, T. Kawamoto, E. Asano and T. Kuroda,
Development of Negative-Ion-Based Neutral Beam Injector for the Large Helical Device; Sep. 1996 (IAEA-CN-64/GP-9)

NIFS-442 K. Toi, K.N. Sato, Y. Hamada, S. Ohdachi, H. Sakakita, A. Nishizawa, A. Ejiri, K. Narihara, H. Kuramoto, Y. Kawasumi, S. Kubo, T. Seki, K. Kitachi, J. Xu, K. Ida, K. Kawahata, I. Nomura, K. Adachi, R. Akiyama, A. Fujisawa, J. Fujita, N. Hiraki, S. Hidekuma, S. Hirokura, H. Idei, T. Ido, H. Iguchi, K. Iwasaki, M. Isobe, O. Kaneko, Y. Kano, M. Kojima, J. Koog, R. Kumazawa, T. Kuroda, J. Li, R. Liang, T. Minami, S. Morita, K. Ohkubo, Y. Oka, S. Okajima, M. Osakabe, Y. Sakawa, M. Sasao, K. Sato, T. Shimpo, T. Shoji, H. Sugai, T. Watari, I. Yamada and K. Yamauti,
Studies of Perturbative Plasma Transport, Ice Pellet Ablation and Sawtooth Phenomena in the JIPP T-IIU Tokamak; Sep. 1996 (IAEA-CN-64/A6-5)

NIFS-443 Y. Todo, T. Sato and The Complexity Simulation Group,
Vlasov-MHD and Particle-MHD Simulations of the Toroidal Alfvén Eigenmode; Sep. 1996 (IAEA-CN-64/D2-3)

NIFS-444 A. Fujisawa, S. Kubo, H. Iguchi, H. Idei, T. Minami, H. Sanuki, K. Itoh, S. Okamura, K. Matsuoka, K. Tanaka, S. Lee, M. Kojima, T.P. Crowley, Y. Hamada, M. Iwase, H. Nagasaki, H. Suzuki, N. Inoue, R. Akiyama, M. Osakabe, S. Morita, C. Takahashi, S. Muto, A. Ejiri, K. Ida, S. Nishimura, K. Narihara, I. Yamada, K. Toi, S. Ohdachi, T. Ozaki, A. Komori, K. Nishimura, S. Hidekuma, K. Ohkubo, D.A. Rasmussen, J.B. Wilgen, M. Murakami, T. Watari and M. Fujiwara,
An Experimental Study of Plasma Confinement and Heating Efficiency through the Potential Profile Measurements with a Heavy Ion Beam Probe in the Compact Helical System; Sep. 1996 (IAEA-CN-64/C1-5)

NIFS-445 O. Motojima, N. Yanagi, S. Imagawa, K. Takahata, S. Yamada, A. Iwamoto, H. Chikaraishi, S. Kitagawa, R. Maekawa, S. Masuzaki, T. Mito, T. Morisaki, A. Nishimura, S. Sakakibara, S. Satoh, T. Satow, H. Tamura, S. Tanahashi, K. Watanabe, S. Yamaguchi, J. Yamamoto, M.Fujiwara and A. Iiyoshi,
Superconducting Magnet Design and Construction of LHD; Sep. 1996 (IAEA-CN-64/G2-4)